

SUPPORTING INFORMATION

Accelerating Charge Transfer in a Triphenylamine-Subphthalocyanine Donor Acceptor System

Anaïs Medina, Christian G. Claessens, G. M. Aminur Rahman, Al Mokhtar Lamsabhi, Otilia Mó, Manuel Yáñez, Dirk M. Guldi and Tomás Torres

General.....	S2
Compound 2.....	S4
Compound 3.....	S9
Compound 1.....	S15
Selected photophysical data for 1, 3 and 4b	S24
Computational details.....	S28
Electrochemical data for 1, 3 and 4b.....	S32

General. Chemicals were purchased from Aldrich Chemical Co., Merck, Acros Organics or Fluka Chemie, used as received unless indicated otherwise.

Most solvents were purchased from SDS. Dry solvents were prepared using molecular sieves (irradiated with microwaves and dried under vacuum).

Monitoring of reactions and purification procedures was performed by TLC, employing silica gel 60 F₂₅₄ plates (Merck). Isolation and purification of most products was carried out by flash column chromatography, using silica gel Merck-60 (230-400 mesh, 0.040-0.063 mm).

Nuclear magnetic resonance (NMR) spectra (¹H and ¹³C) were recorded with a BRUKER AC-200 (200 MHz) or a BRUKER AC-300 (300 MHz) instrument.

Mass spectra (MS) were carried out at the SIdI, using the MALDI technique in a Bruker REFLEX III spectrometer, using dithranol (1,8,9-anthracenetriol) or TCNQ (tetracyanoquinodimethane) as matrix. High resolution (HR-MS) measurements were performed in the same conditions, or using ion bombardment (LSI-MS) in a VG AutoSpec equipment, with *m*-nitrobenzylic alcohol as matrix.

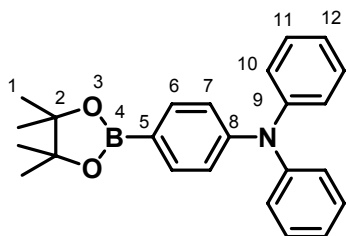
UV/Vis spectra were recorded in a Hewlett-Packard 8453 equipment. Solvents used (mostly CHCl₃) were purchased from Fluka Chemie. The logarithm of the molar absorption coefficient (ϵ) is indicated in parenthesis.

Infrared spectra (IR) were measured on a Bruker Vector 22 spectrophotometer, employing in all cases solid samples in KBr compacted disks.

Electrochemical measurements were performed on an Autolab PGStat 30 equipment using a three electrode configuration system. The measurements were carried out using THF solutions containing 0.1 M tetrabutylammonium hexafluorophosphate (TBAPF₆). A glassy carbon electrode (3 mm diameter) was used as the working electrode, and a platinum wire and an Ag/AgNO₃ (in CH₃CN) electrode were employed as the counter and the reference electrodes, respectively. Ferrocene (Fc) was added as an internal reference and all the potentials were given relative to the Fc/Fc⁺ couple. Both the counter and the reference electrodes were directly immersed in the electrolyte solution. The surface of the working electrode was polished with commercial alumina prior to use. Solutions were stirred and deaerated by bubbling argon for a few minutes prior to each voltammetric measurement. Unless otherwise specified the scan rate was 100 mV/s.

Femtosecond transient absorption studies were performed with 580 nm laser pulses (1 kHz, 150 fs pulse width) from an amplified Ti:Sapphire laser system (Model CPA 2101, Clark-MXR Inc.) equipped with a NOPA-Plus.Nanosecond Laser Flash Photolysis experiments were performed with laser pulses from a Quanta-Ray CDR Nd:YAG system (532 nm, 6 ns pulse width) in a front face excitation geometry. Fluorescence lifetimes were measured with a Laser Strobe Fluorescence Lifetime Spectrometer (Photon Technology International) with 337 nm laser pulses from a nitrogen laser fiber-coupled to a lens-based T-formal sample compartment equipped with a stroboscopic detector. Details of the Laser Strobe systems are described on the manufacture's web site, <http://www.pti-nj.com>. Emission spectra were recorded with a SLM 8100 Spectrofluorometer. The experiments were performed at room temperature. Each spectrum represents an average of at least 5 individual scans, and appropriate corrections were applied whenever necessary. Pulse radiolysis experiments were performed by utilizing 50-ns pulses of 8 MeV electrons from a Model TB-8 / 16-1S Electron Linear Accelerator. Details on such equipment, in general, and the data analysis have been described elsewhere [G. L. Hug, Y. Wang, C. Schöneich, P.-Y. Jiang, R. W. Fessenden, *Radiat. Phys. Chem.* **1999**, *54*, 559.]

2-(4-diphenylaminophenyl)-4,4,5,5-tetramethyl-1,3,2-dioxaborolane 2



n-BuLi (0.48 ml (2.5 M in Hexane), 1.2 mmol) was added dropwise to a solution of 4-bromotriphenylamine (259 mg, 0.8 mmol) in freshly dried and degassed THF (1 mL) at -78 °C under Ar. After 30 min at -78°C, 2-Isopropoxy-4,4,5,5-tetramethyl-1,3,2-dioxaborolane (0.25 mL, 1.19 mmol) was added over 20 minutes to this solution with a syringe. After 90 minutes at -78°C the temperature was raised to room temperature and the mixture was stirred for an additional 4 hours. Then, the solvent was evaporated and the reaction mixture was purified by column chromatography on silica gel using hexane / ethyl acetate (5:1) as eluent. Pinacol boronate **2** was obtained as a colourless oil: 200 mg (67%). ^1H NMR (300 MHz, CDCl_3): δ = 7.67 (d, 2H, H-6), 7.24 (t, 4H, H-11), 7.10 (d, 4H, H-10), 7.03 (d, 2H, H-12), 7.02 (d, 2H, H-7), 1.22 (s, 12H, H-1) ppm. ^{13}C NMR (75.5 MHz, CDCl_3): δ = 150.8 (C-5), 147.3 (C-8, C-9), 135.8 (C-6), 129.3 (C-11), 125.4 (C-10), 123.7 (C-12), 122.1 (C-7), 83.8 (C-2), 20.0 (C-1) ppm. MS (FAB, *m*-NBA): m/z = 371.3 [M] $^+$. HRMS calcd for $\text{C}_{24}\text{H}_{26}\text{NO}_2$: 371.2057; found, 371.2070. FT-IR (KBr): ν = 2973, 2928, 1593, 1495, 1390, 1328, 1162, 1092, 964, 698 cm^{-1} . Anal. Calcd for $\text{C}_{24}\text{H}_{26}\text{BNO}_2$: C, 77.64; H, 7.06; N, 3.77, Found: C, 77.55; H, 7.14; N, 3.62.

$^1\text{H-NMR}$ (CDCl_3 , 300 MHz)

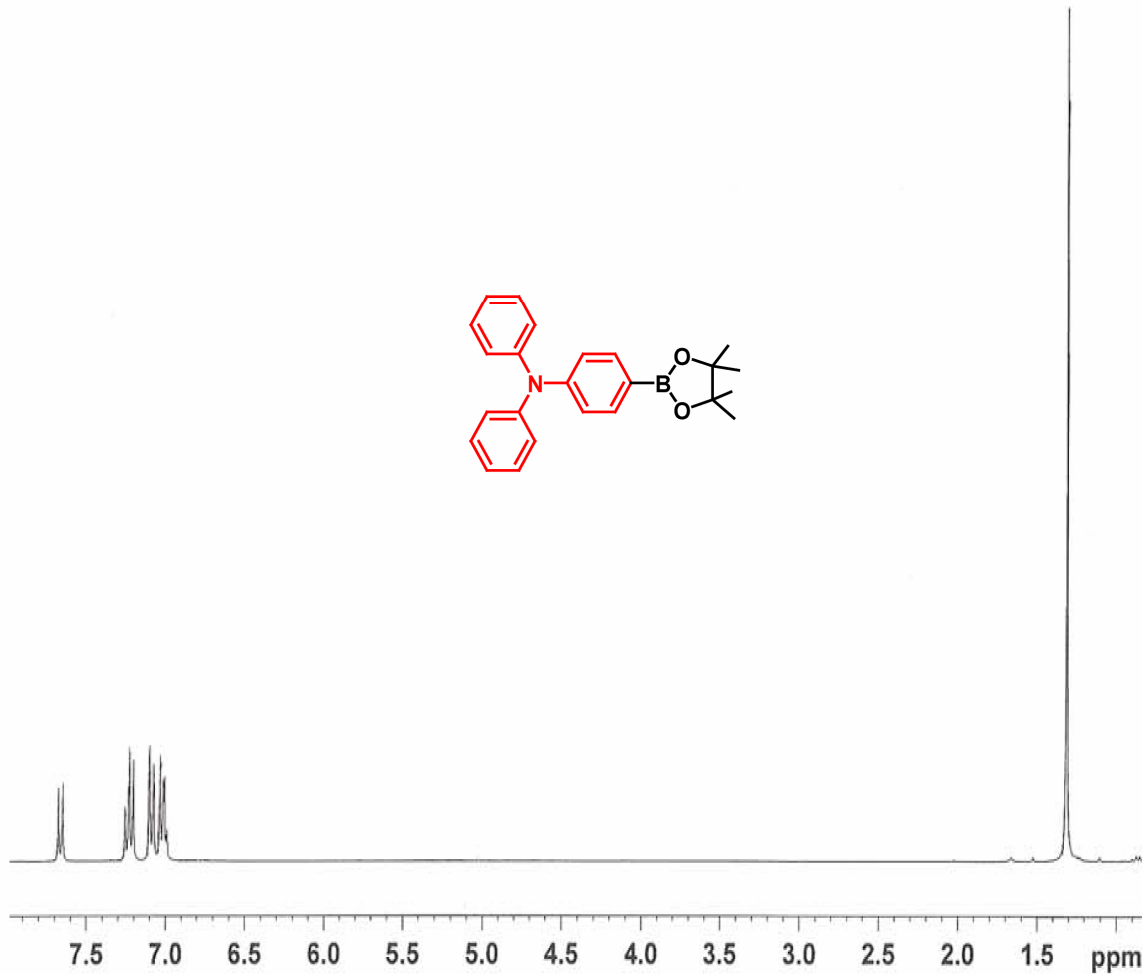


Figure S1

¹³C-NMR (CDCl₃, 75.5 MHz)

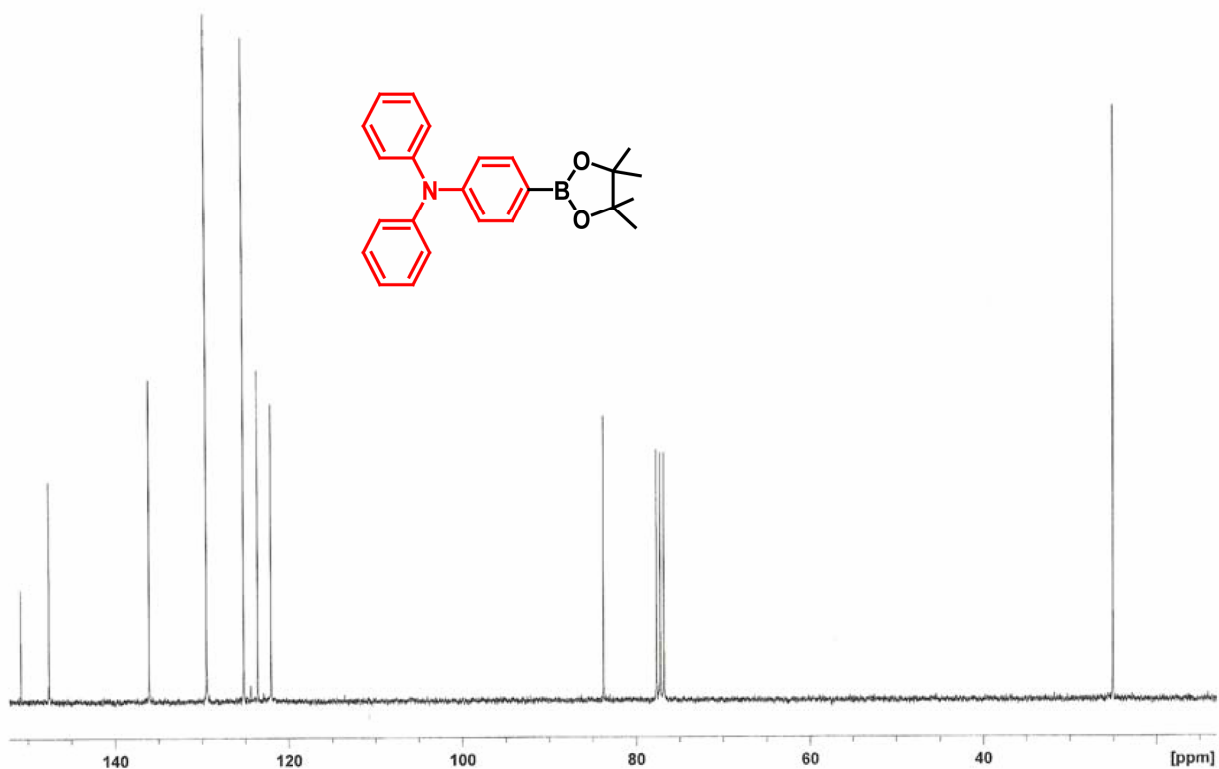


Figure S2

FAB-MS (*m*-NBA) and inset: FAB-HRMS (*m*-NBA)

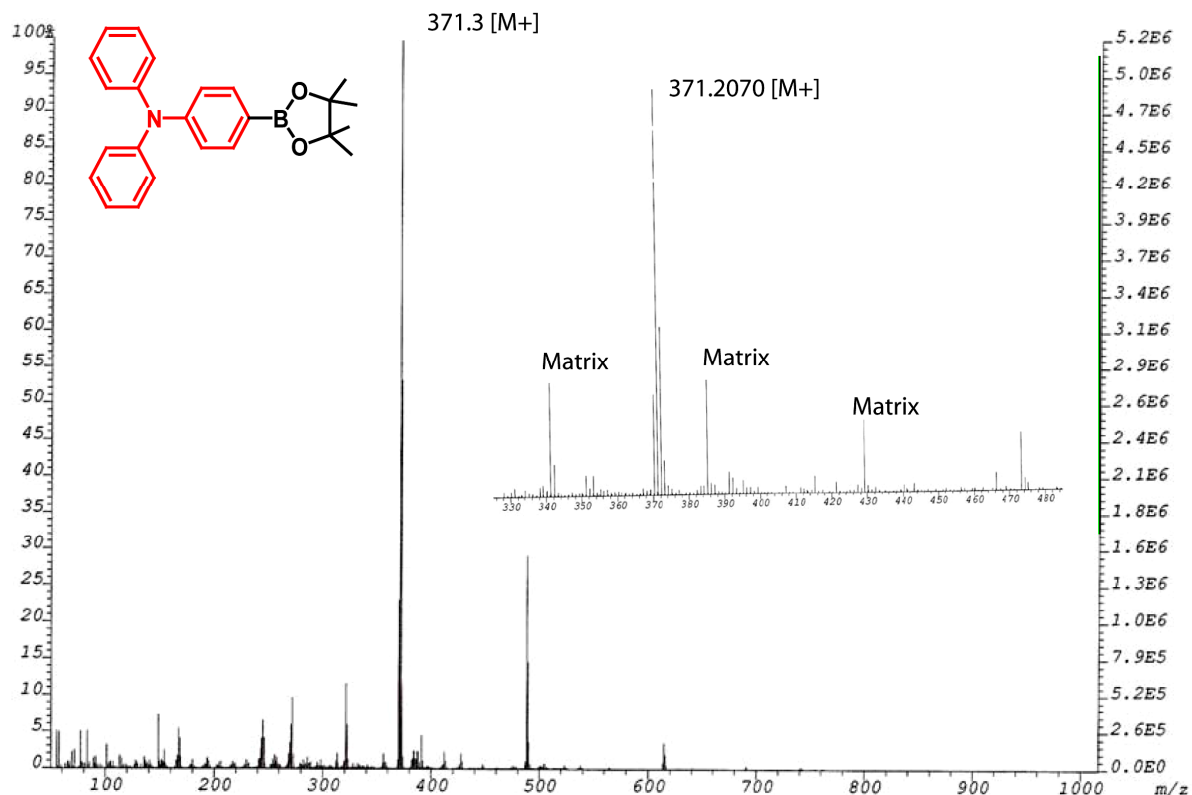


Figure S3

FT-IR (KBr)

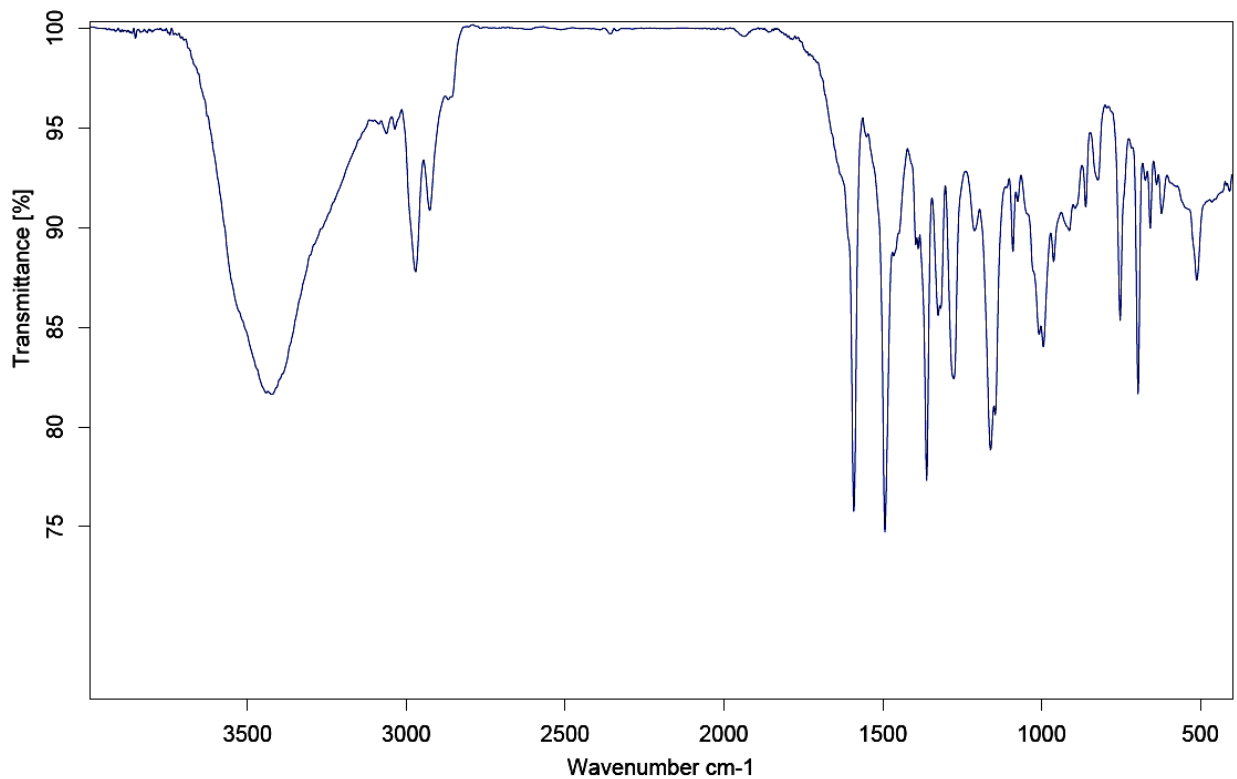
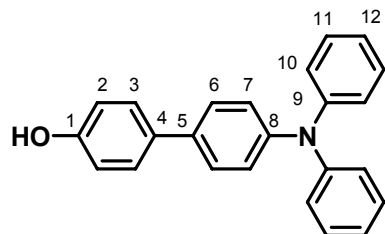


Figure S4

4'-Diphenylamine-[1,1'-biphenyl]-4-ol 3.



4'-Diphenylamine-[1,1'-biphenyl]-4-ol 3. A solution of 4-iodophenol (150 mg, 0.68 mmol), pinacol boronate **2** (278 mg, 0.75 mmol), Pd(PPh₃)₄ (24 mg, 0.02 mmol) and CsF (311 mg, 2.05 mmol) in freshly dried and degassed THF (7 mL) was heated at 70 °C for 2 hour. The reaction was cooled down to room temperature and extracted with CH₂Cl₂. The organic layer was washed with three portions of water and dried over NaSO₄. The brown oil obtained was purified by column chromatography on silica gel using hexane/ ethyl acetate (5:1) as eluent. Phenol **3** was obtained as a yellowish oil: 124 mg (54%). ¹H NMR (300 MHz, CDCl₃): δ = 7.45 (d, 2H, J_0 = 9 Hz, H-3), 7.42 (d, 2H, J_0 = 9 Hz, H-6), 7.26 (t, 4H, J_0 = 9 Hz, H-11), 7.12 (d, 2H, J_0 = 9 Hz, H-7), 7.11 (d, 4H, J_0 = 9 Hz, H-10), 7.02 (d, 2H, J_0 = 9 Hz, H-12), 6.83 (d, 2H, J_0 = 9 Hz, H-2) ppm. ¹³C NMR (75.5 MHz, CDCl₃): δ = 155.3 (C-1), 146.7 (C-9), 138.6 (C-8), 135.5 (C-5), 133.4 (C-4), 129.4 (C-11), 128.1 (C-10), 127.5 (C-6), 124.7 (C7, C-12), 123.1 (C-3), 116.3 (C-2) ppm. MS (FAB, m-NBA): m/z = 337.2 [M]⁺. HRMS calcd for C₂₄H₁₉NO: 337.1467; found, 337.1483. UV-vis (CHCl₃): λ_{max} ($\log \epsilon$) = 317 nm (4.4). FT-IR (KBr): ν = 3441 (OH), 2923, 2851, 1594, 1494, 1326 (C-N), 583 cm⁻¹. Anal. Calcd for C₂₄H₁₉NO: C, 85.43; H, 5.68; N, 4.15, Found: C, 85.32; H, 5.81; N, 4.03.

$^1\text{H-NMR}$ (CDCl_3 , 300 MHz)

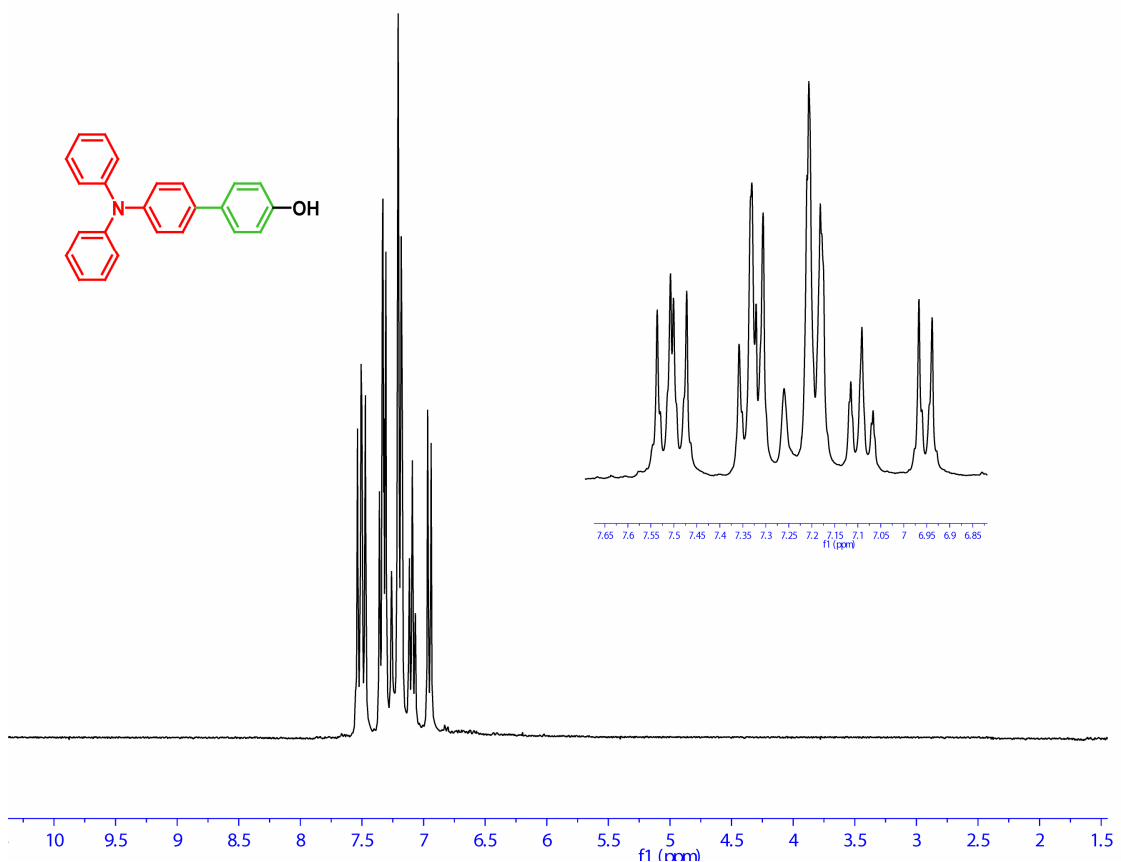


Figure S5

^{13}C -NMR (CDCl_3 , 75.5 MHz)

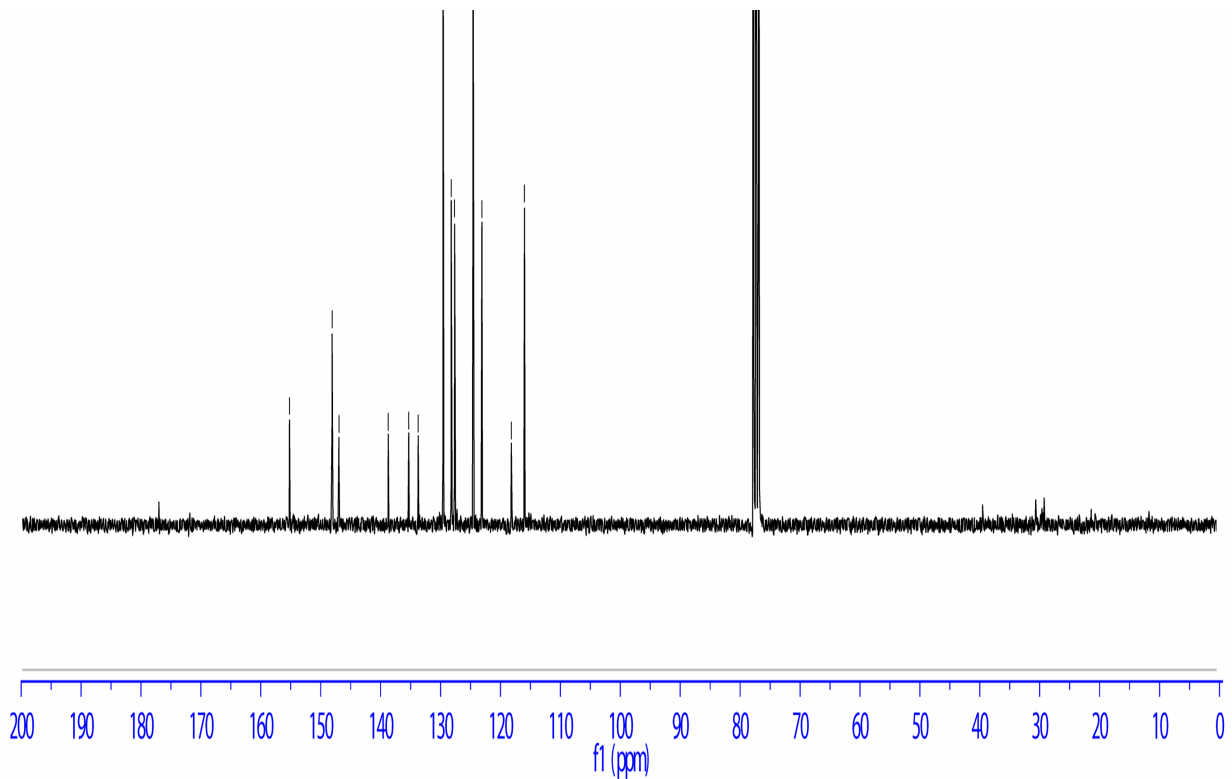


Figure S6

FAB-MS (*m*-NBA) and inset: FAB-HRMS (*m*-NBA)

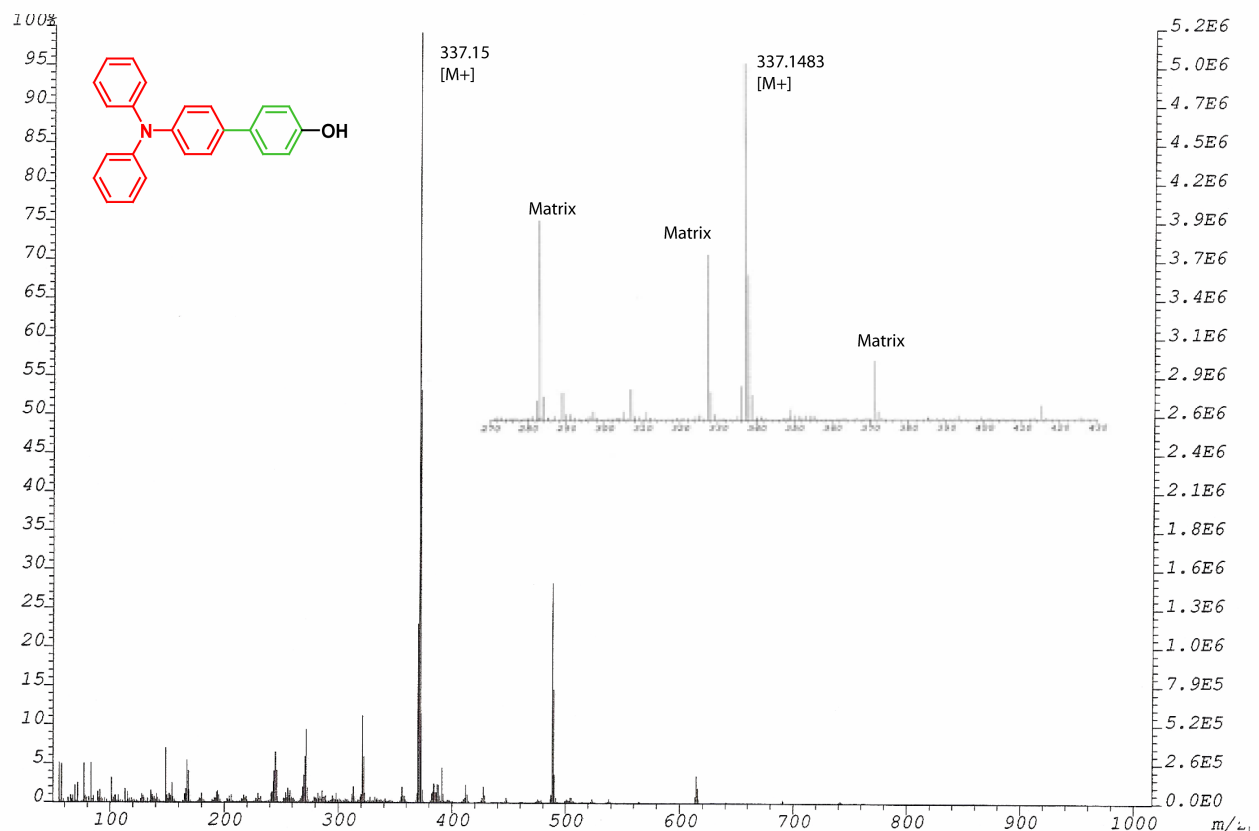


Figure S7

UV-vis (CHCl_3)

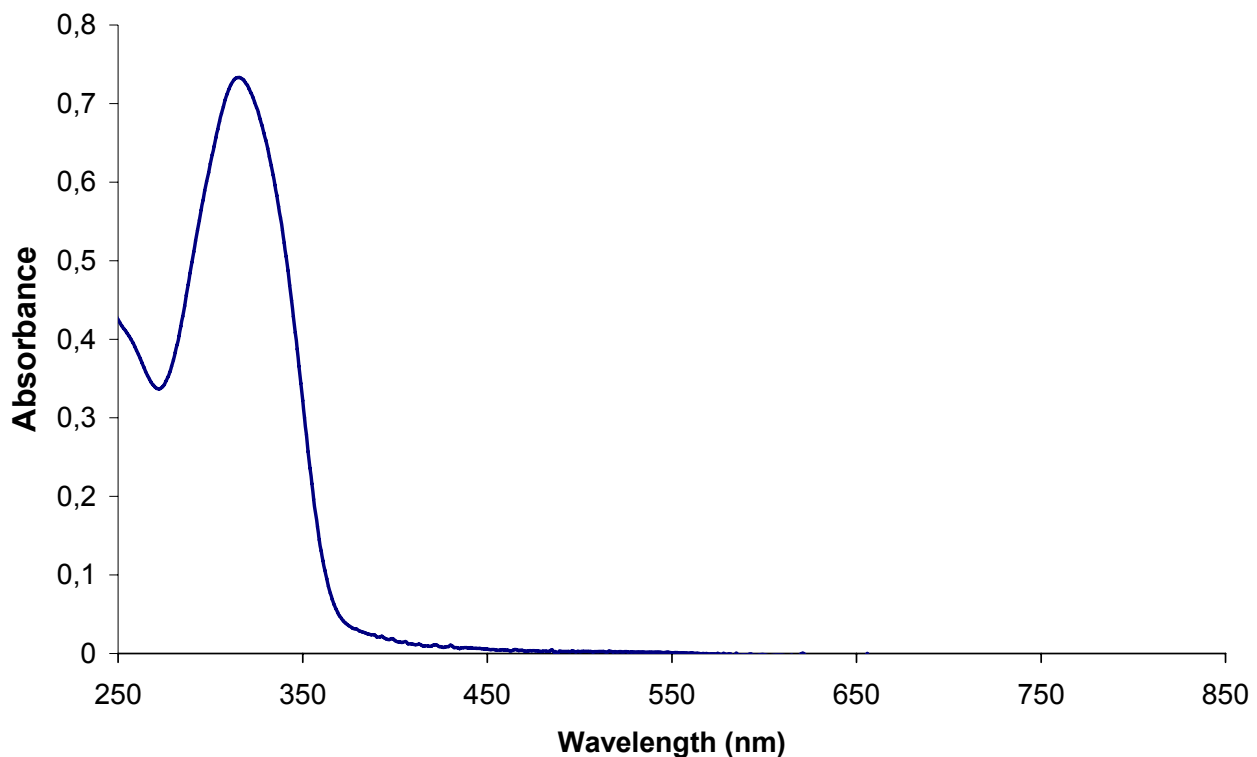


Figure S8

FT-IR (KBr)

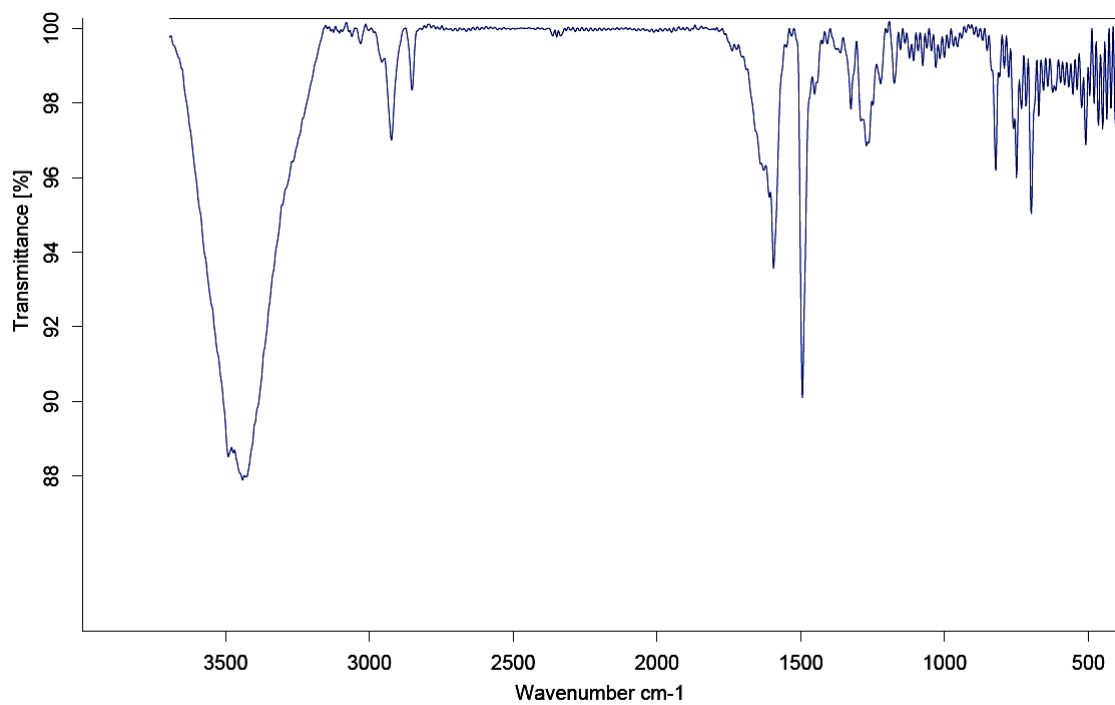
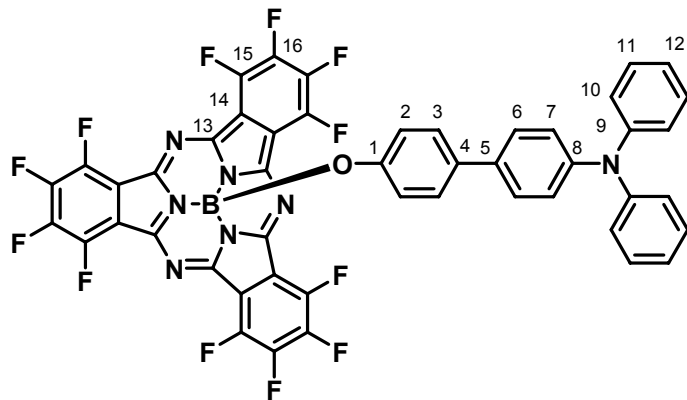


Figure S9

**4'-diphenylamine-[1,1'-biphenyl]-4-oxy-[1,2,3,4,8,9,10,
11,15,16,17,18-dodecafluorosubphthalocyaninato] boron(III) 1.**



**diphenylamine-[1,1'-biphenyl]-4-oxy-[1,2,3,4,8,9,10,
11,15,16,17,18-**

dodecafluorosubphthalocyaninato] boron(III) 1. To a solution of phenol **3** (62 mg, 0.19 mmol) and subphthalocyanine **4** (119 mg, 0.19 mmol) in dry toluene (1 mL) under Ar was added through a syringe NEt₃ (26 µL, 0.19 mmol). The reaction was kept at reflux for 1 hour and cooled down to room temperature. Dichloromethane (50 mL) was added to the reaction mixture and the resulting pink solution was washed with water (15 mL), aqueous HCl (15 mL, 1 M) and finally again with water (15 mL). The organic layer was dried over Na₂SO₄ and evaporated under vacuum. The resulting dark magenta solid was purified by column chromatography on silica gel using hexane / toluene (1:1) as eluent. Subphthalocyanine **1** was isolated as a purple solid 72.5 mg (45%). Mp > 250 °C. ¹H NMR (500 MHz, CDCl₃): δ = 7.15 (t, 4H, H-11), 7.14 (d, 2H, H-12), 6.99 (d, 2H, H-6), 6.98 (d, 2H, H-7), 6.95 (d, 2H, H-3), 6.93 (d, 2H, H-10), 5.32 (d, 2H, H-2) ppm. ¹³C NMR (126 MHz, CDCl₃): δ = 154.9 (C-1), 147.8 (C-15, C-16), 146.7 (C-13), 138.4 (C-9), 135.0 (C-8), 133.4 (C-5), 129.9 (C-4), 129.3 (C-11), 127.9 (C-10), 127.4 (C-12), 124.3 (C-7), 124.2 (C-6), 122.8 (C-3), 117.9 (C-14), 115.7 (C-2)

ppm. ^{19}F NMR (470.5 MHz, CDCl_3): $\delta = -147.38$ (m, 6F), -136.65 (m, 6F) ppm. ^{11}B NMR (160.5 MHz, CDCl_3): $\delta = -15.1$ (s) ppm. MS (FAB, *m*-NBA): $m/z = 947.2$ [M] $^+$, 611.1 [M-axial group] $^+$. HRMS calcd for $\text{C}_{48}\text{H}_{18}\text{BF}_{12}\text{N}_7\text{O}$: 947.1474; found, 947.1454. UV-vis (CHCl_3): λ_{max} ($\log \epsilon$) = 571 (4.6), 552 (sh), 531 (sh), 310 nm (4.4). FT-IR (KBr): $\nu = 3031, 2925, 1534, 1485, 1318, 1032, 881, 680$ cm^{-1} . Anal. Calcd for $\text{C}_{48}\text{H}_{18}\text{BF}_{12}\text{N}_7\text{O}$: C, 60.85; H, 1.91; N, 10.35. Found: C, 60.71; H, 2.00; N, 10.26.

^1H NMR (CDCl_3 , 500 MHz)

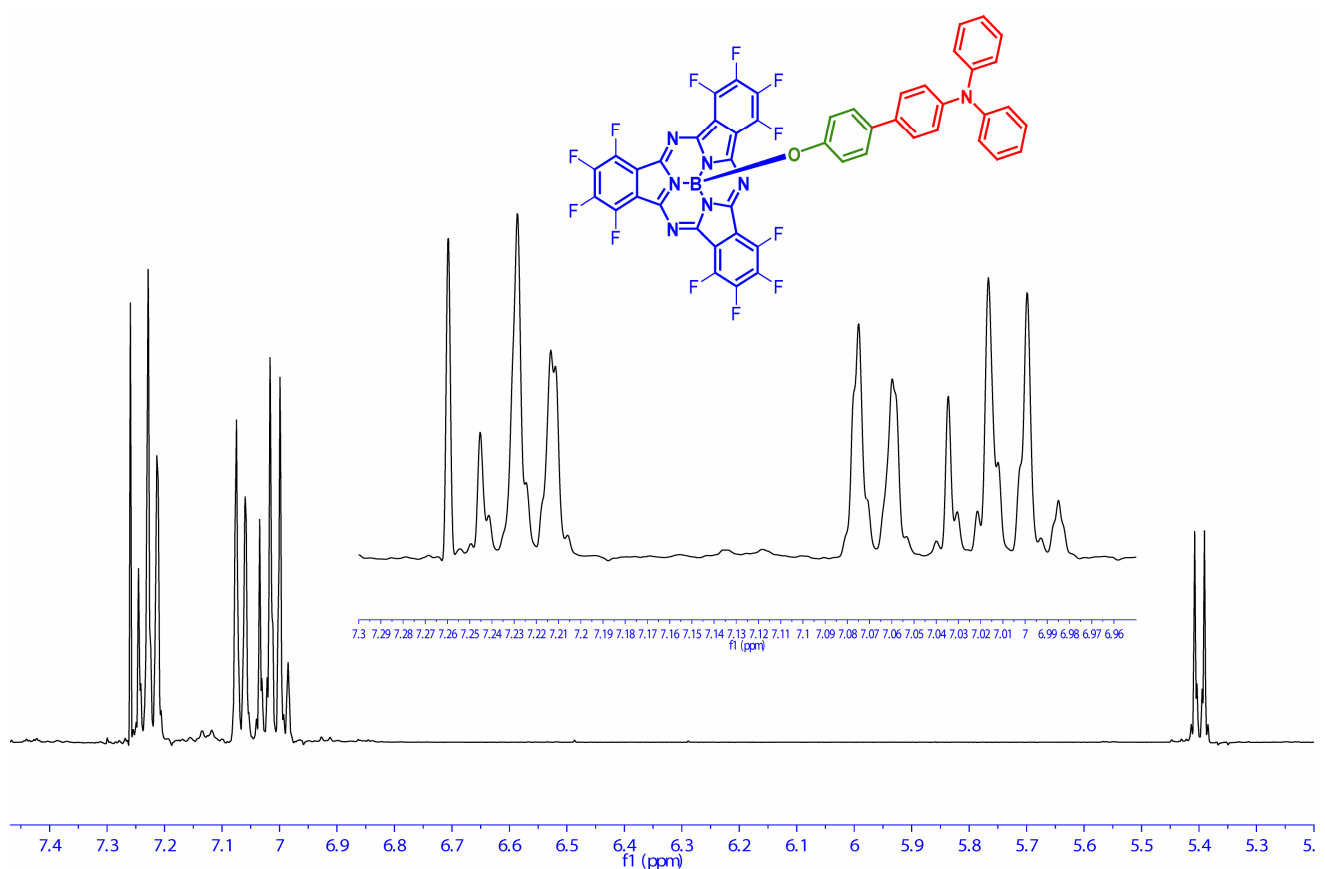


Figure S10

^{13}C NMR (CDCl_3 , 126 MHz)

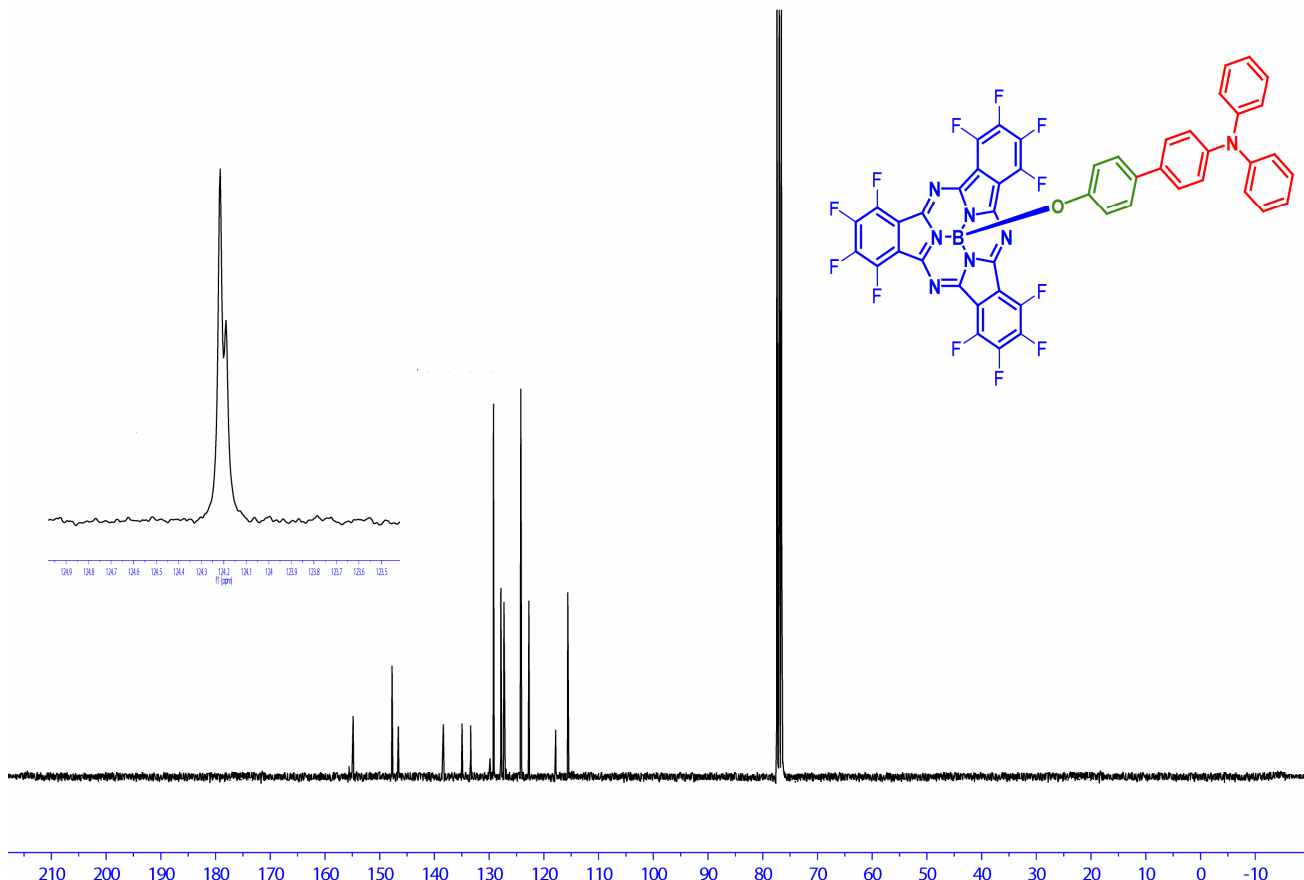


Figure S11

¹⁹F NMR (CDCl₃, 470.5 MHz)

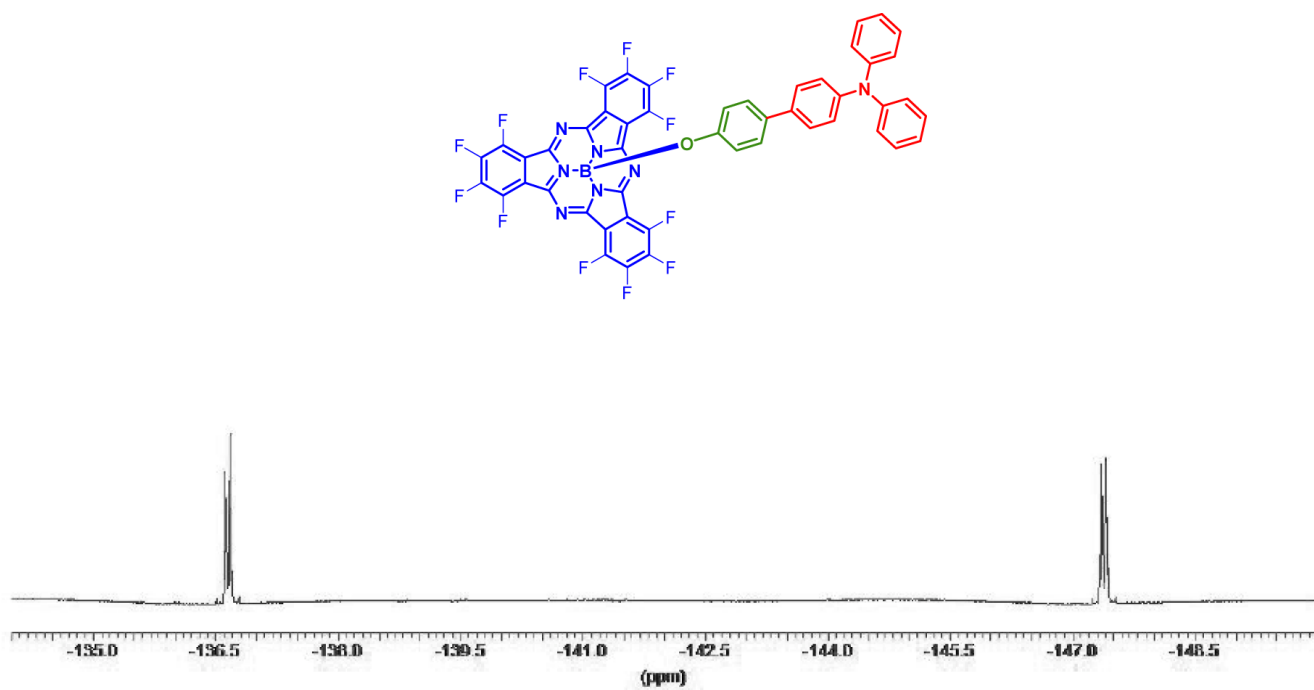


Figure S12

^{11}B NMR (CDCl_3 , 160.5 MHz)

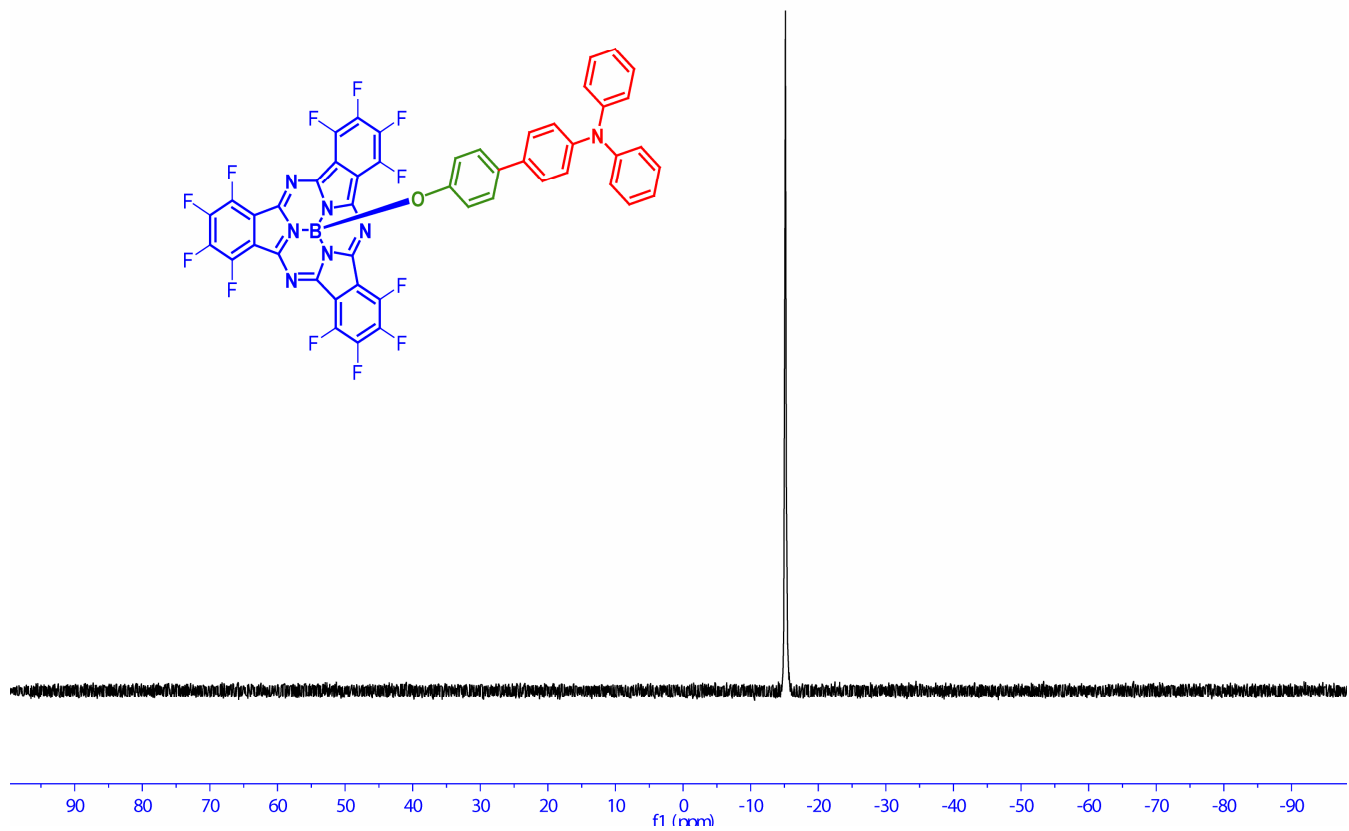


Figure S13

HMQC (^1H : 500 MHz, ^{13}C : 126 MHz, CDCl_3)

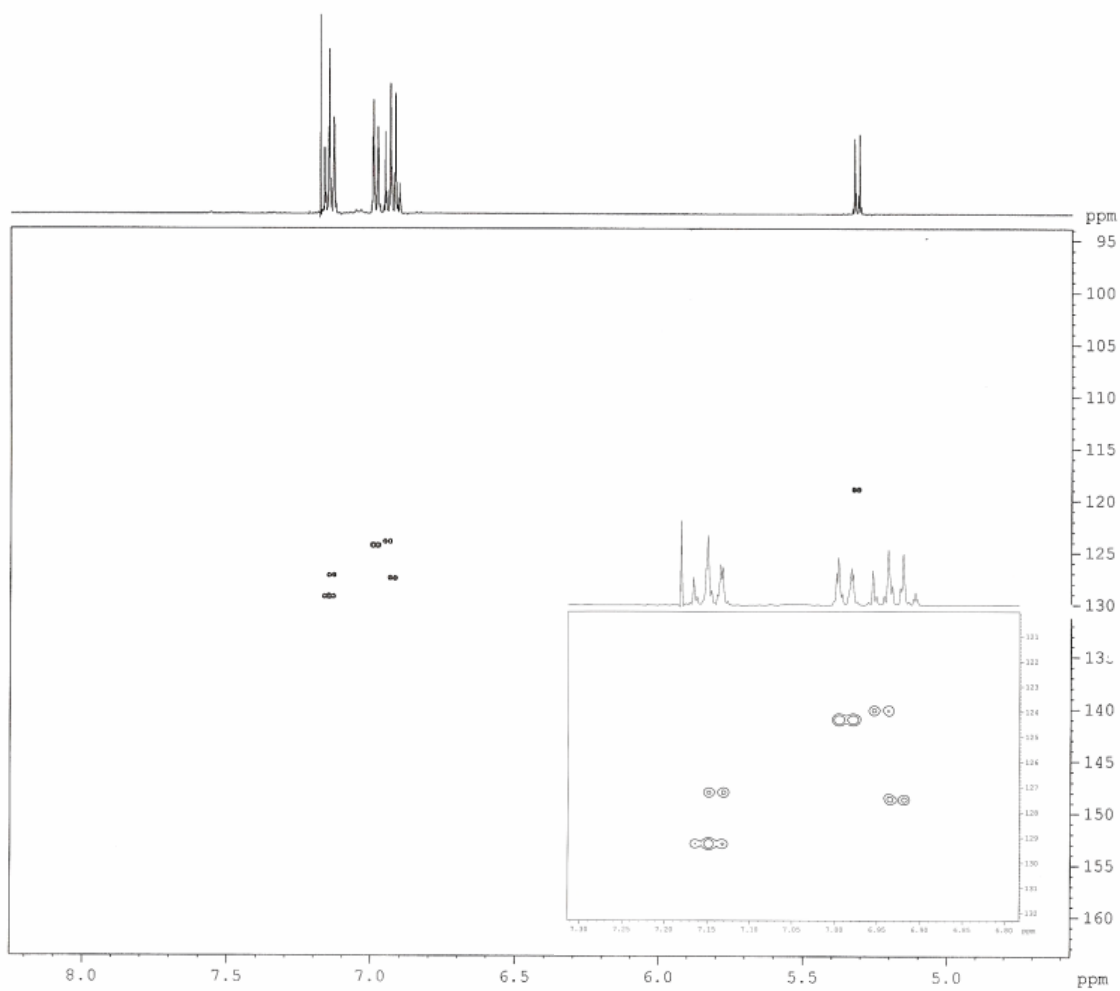


Figure S14

FAB-MS (*m*-NBA) and inset: FAB-HRMS (*m*-NBA)

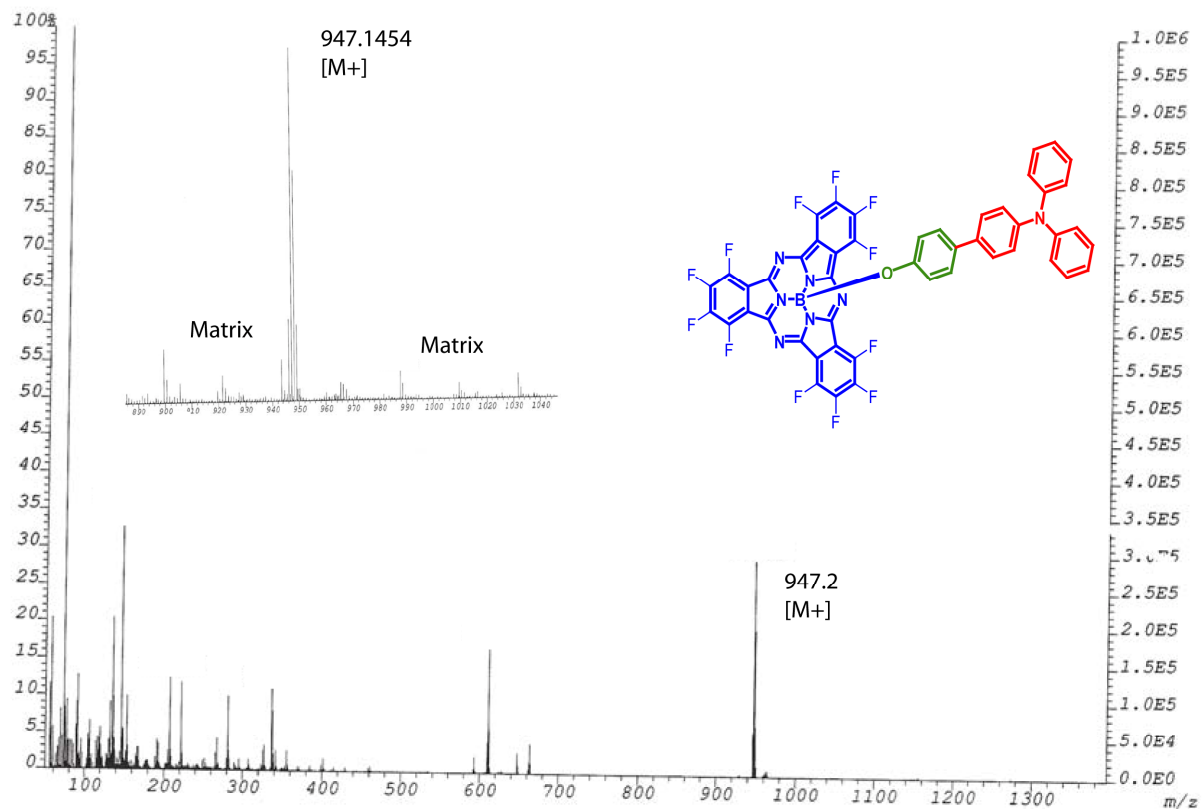


Figure S15

UV-vis (CHCl_3)

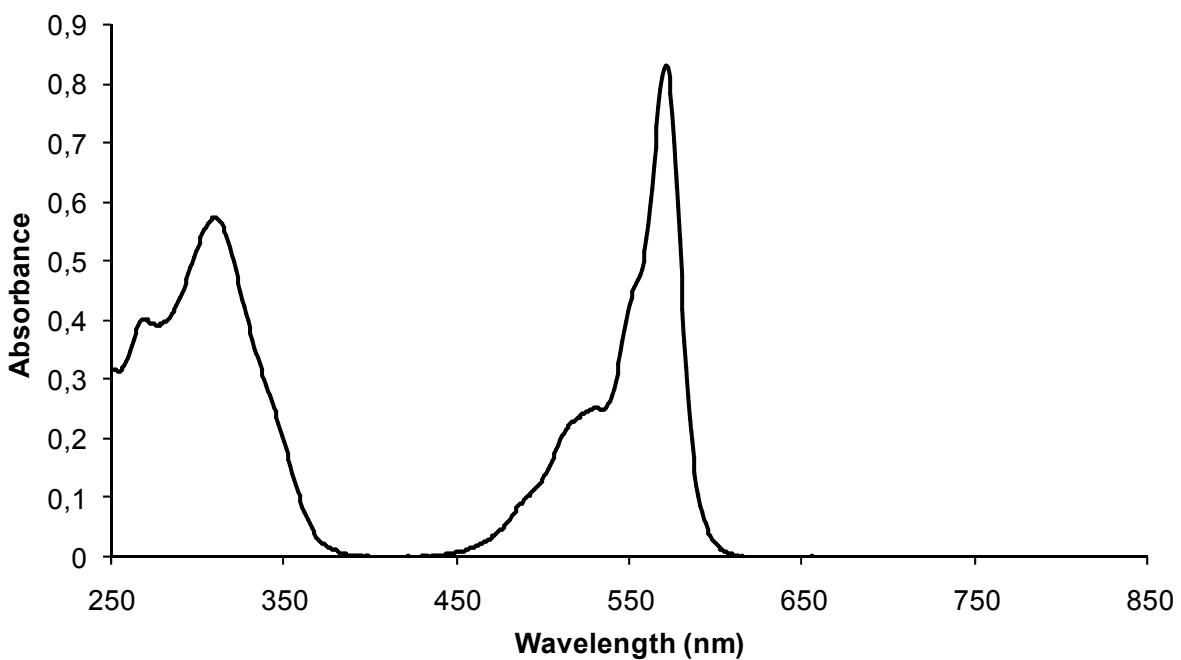


Figure S16

FT-IR (KBr)

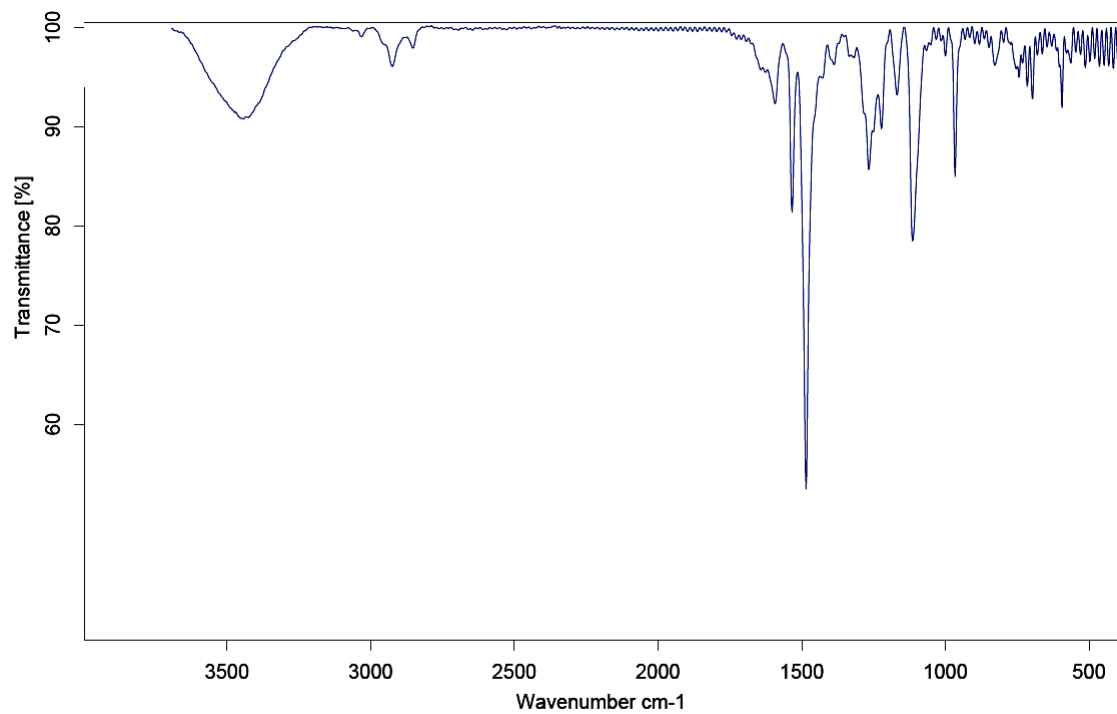


Figure S17

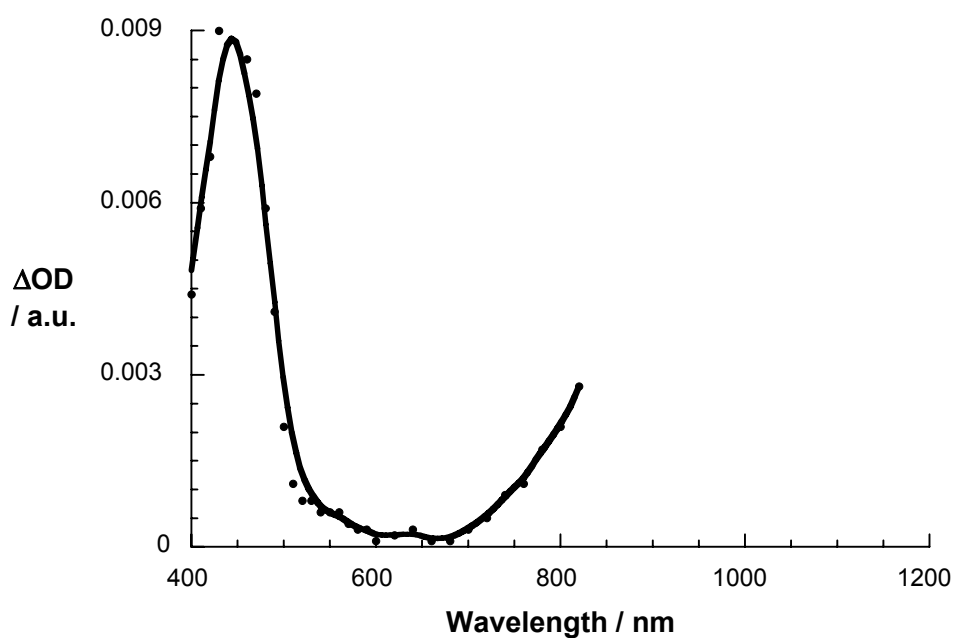
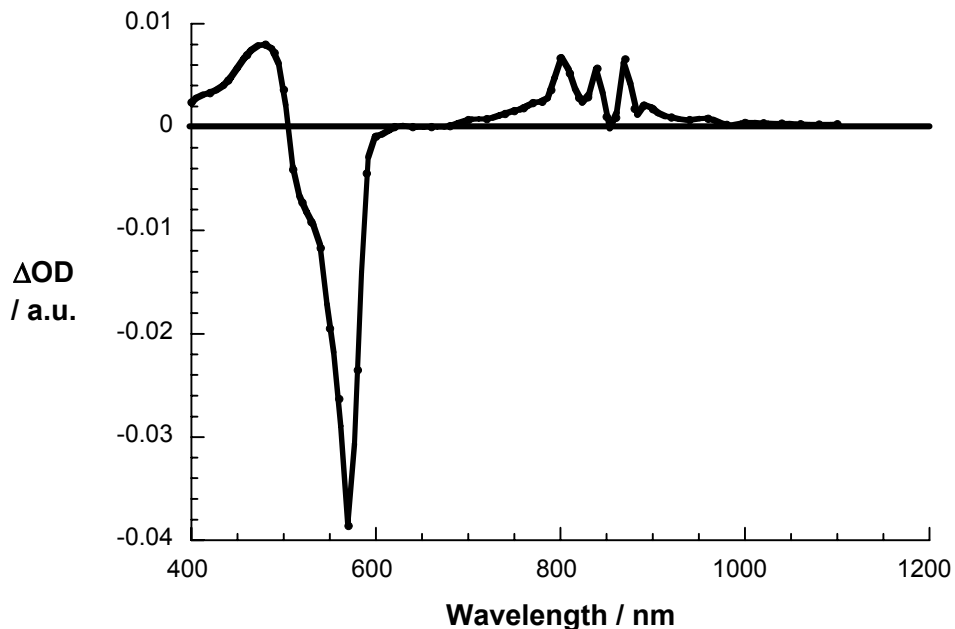


Figure S18: Upper part – differential absorption spectrum (visible and near-infrared) obtained upon femtosecond pulse radiolytic reduction of SubPc **4b** in a deoxygenated solvent mixture containing toluene, 2-propanol and acetone with $(\text{CH}_3)_2\cdot\text{COH}$ and $(\text{CH}_3)_2\cdot\text{CO}^-$ radicals with a time delay of 200 μs at room temperature. Lower part – differential absorption spectrum (visible and near-infrared) obtained upon femtosecond pulse radiolytic oxidation of TPA derivative **3** in oxygenated dichloromethane with $\cdot\text{OOCCH}_2\text{Cl}$ or $\cdot\text{OOCCHCl}_2$ radicals with a time delay of 200 μs at room temperature.

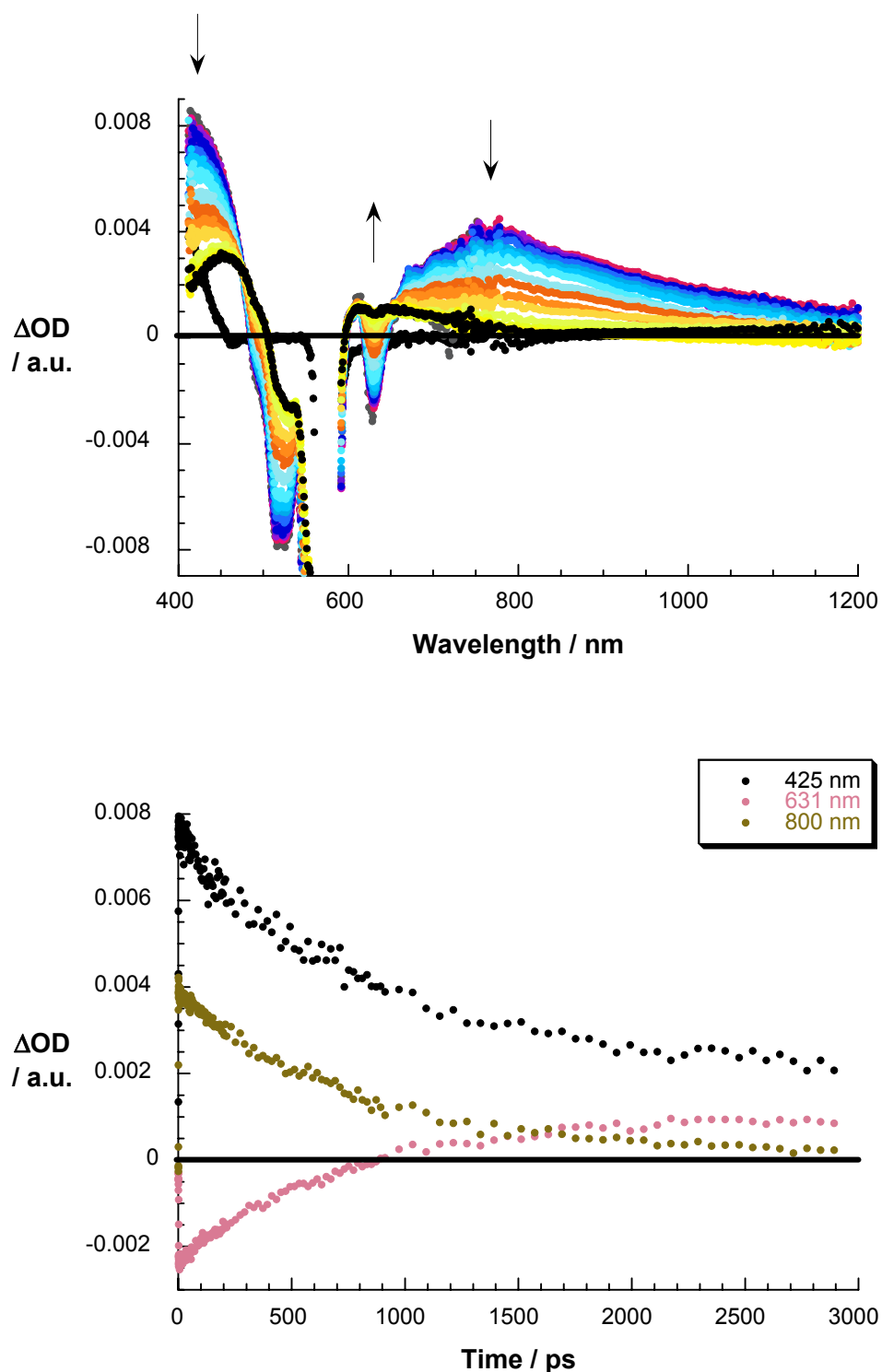


Figure S19: Upper part – differential absorption spectrum (visible and near-infrared) obtained upon femtosecond flash photolysis (580 nm) of SubPc **4b** in nitrogen saturated toluene with several time delays between 0 and 3000 ps at room temperature. Lower part – time-absorption profiles of the spectra shown above at 425, 631 and 800 nm, monitoring the formation and decay of the SubPc **4b** singlet excited state.

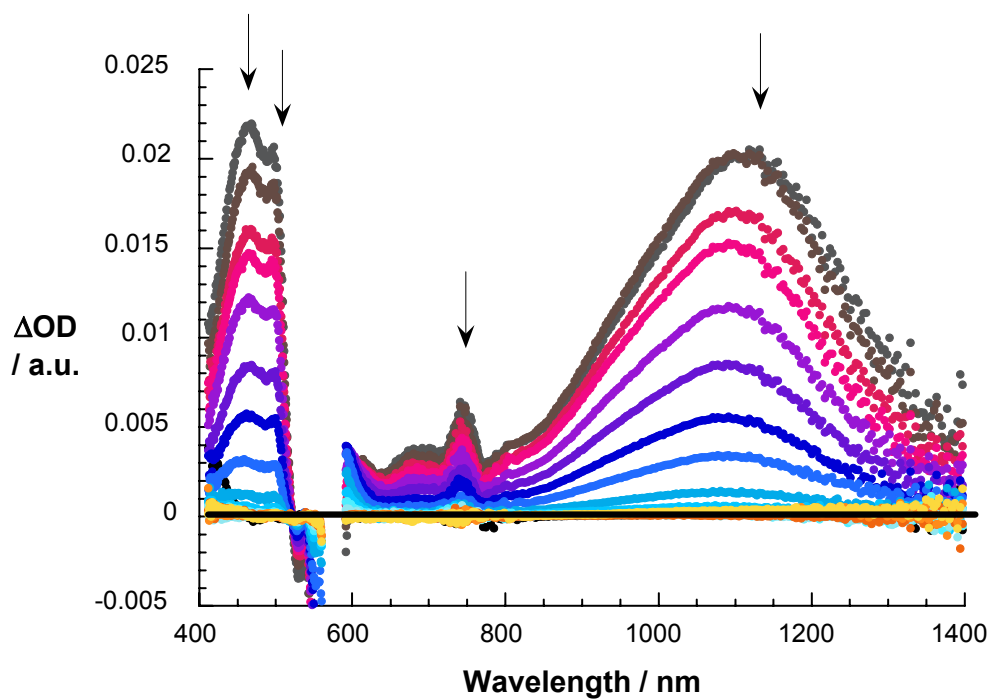
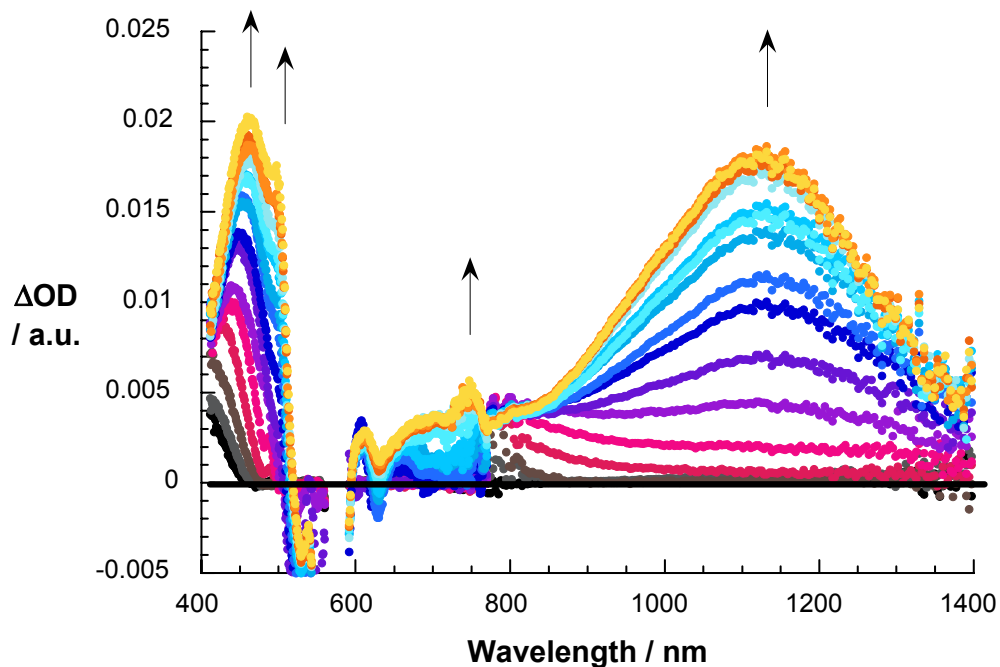


Figure S20: Upper part – differential absorption spectrum (visible and near-infrared) obtained upon femtosecond flash photolysis (580 nm) of SubPc-TPA **1** in nitrogen saturated toluene with several time delays between 0 and 5 ps at room temperature. Lower part – differential absorption spectrum (visible and near-infrared) obtained upon femtosecond flash photolysis (580 nm) of SubPc-TPA dyad **1** in nitrogen saturated toluene with several time delays between 5 and 60 ps at room temperature.

Computational Details: The structure of dyad **1** (See Table S1) has been fully optimized using the B3LYP density functional (DFT) approach together with a 6-31G(d) basis set expansion. The hybrid B3LYP method, combines the Becke's three-parameter nonlocal hybrid exchange potential with the nonlocal correlation functional of Lee, Yang and Parr, and it has been shown to yield reliable geometries for a wide variety of systems. For all the stationary points found, the corresponding harmonic vibrational frequencies were calculated at the same level of theory used for the geometry optimization in order to ensure that they corresponded to local minima of the potential energy surface.

Using these optimized geometries the excited states and the absorption bands in the UV-visible region were calculated by using time-dependent DFT techniques (TDDFT), as implemented in the Gaussian-03 suite of programs and the same functional employed to characterized the corresponding ground state. The calculations have been performed for the spin allowed singlet excited states, and only transitions with oscillator strengths greater than 1.0×10^{-3} have been considered and therefore analyzed. Among them only those associated with the formation of a charge-separation state are of relevance in this study and therefore were the only ones analyzed.

Table S1. B3LYP/6-31G(d) optimized geometry (Cartesian coordinates in Å) for SubPc-TPA 1

6	0	2.827408	3.317708	0.464274
6	0	1.956025	2.768133	1.462172
6	0	1.548629	3.547852	2.541375
6	0	1.982414	4.868258	2.619857
6	0	2.835130	5.406156	1.643266
6	0	3.270152	4.633584	0.570180
6	0	3.152563	2.241726	-0.461021
6	0	1.759658	1.363528	1.133886
7	0	1.373413	0.340102	1.907209
7	0	2.363735	1.188656	-0.081658
7	0	4.185090	2.110114	-1.304857
6	0	1.739697	-0.889044	1.520473
6	0	3.113318	-2.271962	0.313928
6	0	1.912789	-2.107149	2.298657
6	0	2.772168	-2.972487	1.543844
6	0	1.494521	-2.475691	3.574469
6	0	3.192314	-4.185295	2.083518
6	0	1.905582	-3.701822	4.089772
6	0	2.746549	-4.548744	3.351159
6	0	4.534397	0.864486	-1.655193
6	0	4.514728	-1.395202	-1.267192
6	0	5.809922	0.338267	-2.119575
6	0	5.797644	-1.075624	-1.876745
6	0	6.955564	0.952314	-2.618345
6	0	6.931366	-1.840073	-2.138698
6	0	8.072543	0.169478	-2.896372
6	0	8.060557	-1.213790	-2.658773
7	0	3.793730	-0.234803	-1.320284
7	0	2.343717	-1.139443	0.318238
7	0	4.145419	-2.446703	-0.522582
5	0	2.384751	-0.135382	-0.810765
8	0	1.447926	-0.311579	-1.873518
6	0	0.087291	-0.276824	-1.674227
6	0	-0.617650	-1.459335	-1.427705
6	0	-0.611177	0.930838	-1.774994
6	0	-2.001211	-1.427285	-1.271630
1	0	-0.073300	-2.396822	-1.363778
6	0	-1.995190	0.951285	-1.620440
1	0	-0.064809	1.841718	-2.000844
6	0	-2.721943	-0.223790	-1.361559
1	0	-2.529736	-2.351402	-1.054898
1	0	-2.525121	1.893107	-1.731971
6	0	-4.195634	-0.195400	-1.197438
6	0	-5.006768	-1.236718	-1.680229
6	0	-4.839443	0.874723	-0.552729
6	0	-6.388117	-1.219170	-1.520580
1	0	-4.549944	-2.072969	-2.202276
6	0	-6.221698	0.912199	-0.404910
1	0	-4.246543	1.690258	-0.147830
6	0	-7.020883	-0.139199	-0.883220
1	0	-6.986779	-2.040765	-1.900477
1	0	-6.689557	1.755073	0.093474
7	0	-8.430714	-0.111064	-0.726852
6	0	-9.274517	-0.567058	-1.777426
6	0	-10.398181	-1.360274	-1.494582
6	0	-8.998841	-0.229211	-3.112301
6	0	-11.228859	-1.795735	-2.525320
1	0	-10.614216	-1.630418	-0.465808

6	0	-9.824997	-0.685000	-4.137885
1	0	-8.136470	0.389949	-3.338212
6	0	-10.946814	-1.466366	-3.852794
1	0	-12.094327	-2.408898	-2.287768
1	0	-9.596300	-0.413651	-5.165259
1	0	-11.592568	-1.813670	-4.654252
6	0	-9.005345	0.375837	0.479972
6	0	-10.129777	1.216198	0.444839
6	0	-8.458966	0.022076	1.724287
6	0	-10.696351	1.682378	1.629649
1	0	-10.553911	1.498804	-0.513422
6	0	-9.021402	0.508384	2.902959
1	0	-7.594484	-0.633269	1.759873
6	0	-10.144971	1.336916	2.865300
1	0	-11.566592	2.331975	1.583394
1	0	-8.585152	0.224235	3.857085
1	0	-10.584991	1.708130	3.786458
9	0	3.999192	-5.009579	1.413322
9	0	3.113706	-5.716793	3.882709
9	0	1.499987	-4.091367	5.300285
9	0	0.704313	-1.690666	4.308068
9	0	6.958114	-3.154828	-1.914873
9	0	9.152854	-1.926501	-2.942472
9	0	9.175855	0.728184	-3.398460
9	0	7.005085	2.265752	-2.845961
9	0	4.088655	5.173433	-0.334368
9	0	3.223957	6.678055	1.756225
9	0	1.587710	5.645761	3.630495
9	0	0.747434	3.065846	3.492611

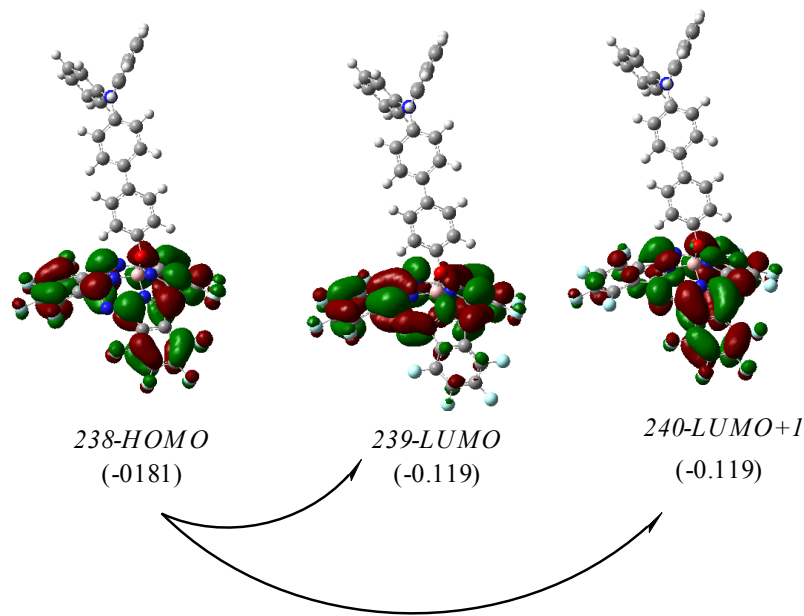


Figure S21. The transitions predicted at 882 and 870 nm, with negligible oscillator strengths, involve transitions from the HOMO to the LUMO and LUMO+1 orbitals, respectively.

Table S2. Redox potentials values for SubPc dyads

Compound ^a	E ¹ _{½red}	E ² _{½red}	E ³ _{red} ^b	E ⁴ _{red} ^{b,c}	E _{oxid} ^b
1	-1.06	-1.71	-2.572		0.617
4b	-1.07	-1.70	-2.451	-2.719	—
3	—	—	—	-2.680	0.549

[a] Experimental conditions: V vs. Fc/Fc⁺, THF as solvent, GCE as working electrode, Pt as counter-electrode, Bu₄NPF₆ (0.1 M) as supporting electrolyte; scan rate 100 mVs⁻¹. The concentration of the sample in all the measurements has been 0.3 mM. [b] These redox processes are irreversible and, hence, only the cathodic and anodic peaks are given. [c] Corresponding to the axial aromatic moieties.

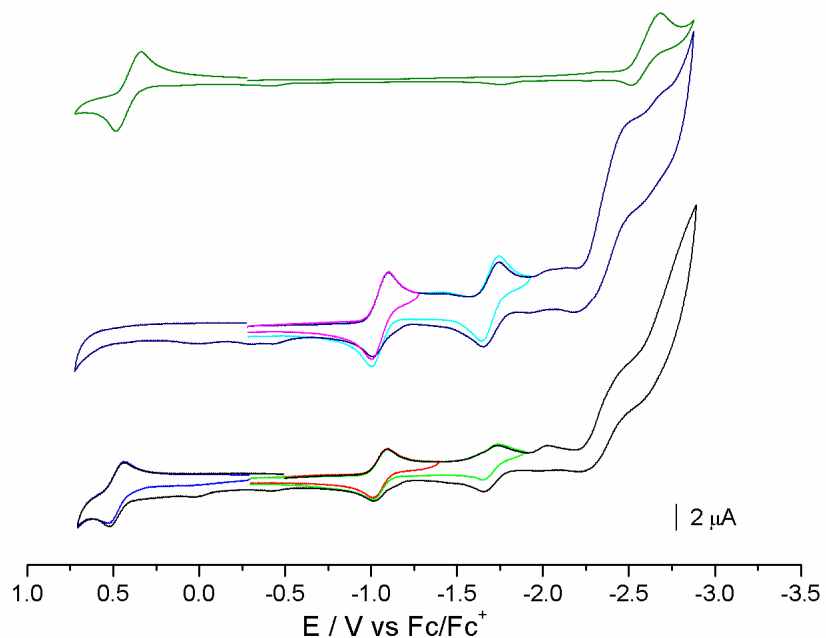


Figure S22. Cyclic Voltammograms (THF, Ag/AgNO₃ as reference electrode, glassy carbon as working electrode, Bu₄NPF₆ as supporting electrolyte, scan rate 100 mV s⁻¹, 298 K) of SubPc conjugates (0.3 mM).